PRAMANA
— journal of
physics

Vol. 59, No. 6
December 2002
pp. 963–976

Cryogenic, superconducting and rf results of the SRFQ2 of PIAVE

A M PORCELLATO[1], G BISOFFI[1], V ANDREEV[1], G BASSATO[1], G BEZZON[1], S CANELLA[1], F CHIURLOTTO[1], A LOMBARDI[1], L BERTAZZO[1], D CONVENTI[1], G GALEAZZI[1], S MARIGO[1], V PALMIERI[1], F POLETTO[1], T SHIRAI[2], S Y STARK[3] and F STIVANELLO[1],

[1]INFN Laboratori Nazionali di Legnaro (Pd), Italy

[2]Nuclear Science Research Facility, ICR, Kyoto University, Kyoto, Japan

[3]Strumenti Scientifici Cinel, Vigonza (Pd), Italy

Abstract. SRFQ2 is the second RFQ superconducting (SC) structure of PIAVE, the positive ion injector of the SC LINAC for heavy ions ALPI, in operation at Legnaro.

During 2001, SRFQ2 was extensively tested at cryogenic temperature reaching its design performance, i.e., 280 kV inter-electrode voltage (equivalent to 25 MV/m peak surface electrical field) at 7 W dissipated power.

This paper describes the treatments, the main difficulties arisen during the tests, the way they were overcome and the measurement sequences that allowed the characterization of SRFQ2 behavior. A brief description of future programs is also given.

Keywords. Positive ion injector; cryogenic rf; RFQs; superconducting resonators.

PACS Nos 29.17.+w; 07.20.Mc

1. Introduction

Two RFQs, housed in one cryostat, are the main and more innovative structures of PIAVE [1,2], which is going to be an effective alternative to the 15 MV XTU tandem as ALPI [3] injector in case of ion species with $A > 100$ and, in general, when larger current have to be delivered to experiments. Table 1 sums up the main design characteristics of the two structures. Both are built in Nb, only the end plates being produced by Nb sputtering on Cu. The RFQs are designed for a minimum q/A ratio of 1/9 ($^{238}U^{28+}$) and they will accelerate the beam coming from an ECR source, located on a 350 kV platform [4], delivering it, at a velocity of 0.0355 c, to an array of eight SC quarter wave resonators (QWRs) housed in two cryostats. They are ready for the final installation at present and have a similar design of low β ALPI resonators, but a reduced β of 0.047, in order to provide a suitable matching with ALPI [5].

The first resonator to be built and tested was SRFQ2, the second in the acceleration line. This not only because it is a factor two smaller in length and so quicker to build than

Table 1. Main features of PIAVE sc RFQ's.

Mass to charge ratio	8.5		
Beam current	<5	μA	
RMS emittance	0.1	mmmrad	norm.
Radio frequency	80	MHz	
Input energy	37.1	keV/u	$\beta = 0.0089$
Peak surface field	25.5	MV/m	
Max. stored energy	≤ 4	J/RFQ	
Band width	>20	Hz	
	SRFQ1	SRFQ2	
Vanes length	137.8	74.61	cm
Output energy	341.7	586	keV/u
Voltage	148	280	kV
Tank diam. (approx.)	65	65	cm
Number of cells	42.6	12.4	
Average aperture R_0	0.8	1.53	cm
Modulation factor m	1.2–3	3	
Synchronous phase	$-40 \div -18$	-12	deg
Dissipated power	<7	<7	W

SRFQ1 [6], but also because it is more critical in terms of stored energy and peak fields, thus making the reaching of the design performance more demanding.

At present the installation of PIAVE cryogenic plants and relative distribution lines are in course. The two QWR cryostats are assembled and ready to be installed. The arrival of the RFQ operation cryostat is foreseen for spring 2002. The first cold test of SRFQ1, the construction of which is completed, will begin soon.

RFQ2 reached its design performance, as described later in this paper, and a final SRFQ2 cold test is scheduled at the beginning of February, before its installation in the PIAVE hall in late spring 2002.

The first results of the commissioning of the low-energy beam transport line (LEBT) are presented elsewhere [7]. We should be ready to deliver the first PIAVE to beam to ALPI at the end of 2002.

2. The SRFQ2 and its test cryostat

The SRFQ2 structure is presented in figure 1.

The design criteria and construction sequence are described in detail in [8,9]. Here only a brief description of the main construction issues, that have had relevance during the rf and cryogenic tests, is presented.

The SRFQ2's four modulated electrodes are rod-type, milled in a computer-controlled machine according to beam dynamics requirements. They are the only resonator parts produced from a thick bar, all the remaining resonator inner parts being made from 3 mm Nb sheet (RRR=250), suitably shaped and electron beam-welded.

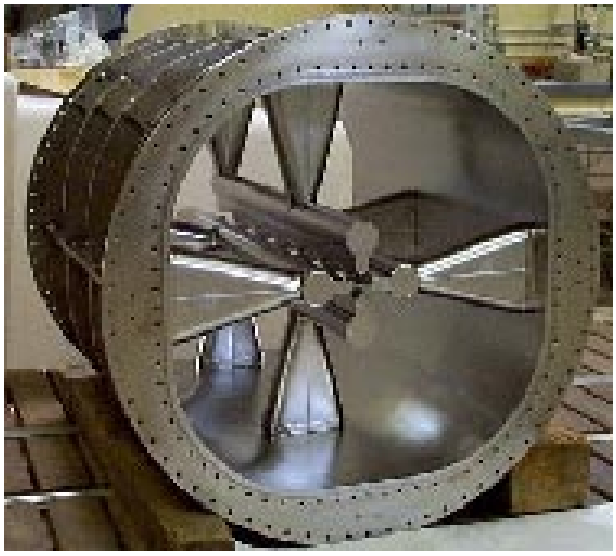

Figure 1. SRFQ2 resonator without ending plates before being assembled into the He tank.

The rods, carved inside, have an empty cylinder welded on their back. This gives to the electrode a vane-type shape, useful to reduce the influence of dangerous multipole modes on beam motion. Two trapezoidal-shaped stems support each electrode. The stems of the horizontal electrodes are placed in an intermediate position with respect to the ones of the vertical electrodes, thus allowing halving of the magnetic field on the rods, on the surface of which the current density is more critical because of the larger thickness of Nb. Another advantage of this stem configuration is the possibility to use the electric field present in both the entrance and exit gaps for beam acceleration [10].

The stems are welded to a Nb outer tank stiffened by Ti ribs. The electrode alignment was checked by bead pulling measurement at 300 K, which showed a field unbalance between quadrants $(\Delta E/E) < 0.4\%$. The measure of frequency splitting of the dipole mode at 4 K resulted in even lower misalignment $(\Delta E/E_{\mathrm{av}}) < 0.34\%$).

The resonator end flanges are made of Nb in the inner part and in Ti in the outer parts. The resonator length is 74 cm; its inner diameter is about 60 cm. The resonator weight is about 300 kg. Two copper plates, the pulling-pushing of which allows the resonator fine-tuning, are close to the resonator body. They are plated with about 2 μm Nb layer using the dc bias sputtered technology developed at Legnaro for QWR sputtering [11]. During the resonator cool down after the sputtering process, nitrogen is introduced in the sputtering chamber producing a surface hardening. There are no gaskets between end plates and resonator flanges, the contact being forced by mechanical levers.

The resonator has three rf ports, 20 mm in diameter, located by the long stem side, at 4 cm distance. First one is for the pick up antenna, the second for the measurement coupler, and the third for the high-power coupler [12]. A fourth port is foreseen for the fast tuner that will be implemented in the final cryostat to enlarge the resonator band width.

All the antennas are of inductive type. It is possible to adjust (and then fix) the pick up position to choose the pick-up Q value most suitable for the measurement condition.

Both measurement and power coupler are movable, with their Q's ranging from $3 \times 10^{+10}$ to $4 \times 10^{+6}$, but only the second one has an rf input line capable to manage the reactive power necessary for phase and amplitude resonator locking.

About 30 diodes (Lakeshore DT470) are screwed (or glued) in various positions on the resonator ribs, inside the electrodes and on the ending plate, so as to monitor the cavity temperature. Their computer controlled visualization was crucial in modulating the rf power during conditioning, thus avoiding thermal transition of some resonator areas.

A few 100 Ω rf loads, mounted on the ribs, are used as heaters for resonator baking and for fast warm up after a measurement cycle.

The resonator outer structure is the inner surface of the liquid He tank of the cryostat. The stem and electrode baking cylinders are parts of the liquid He tank. Two isolated pipes (2 mm internal diameter) acting as siphons, connect the inner part of the lower electrode to the top of the liquid He tank and allow a convenient evacuation of the He gas produced inside the lower electrode [13]. The hydrostatic pressure of the upper liquid He naturally assures gas draining inside the electrode, avoiding the use of forced He flux and related cavity resonance frequency instability. Indium gaskets realize the vacuum sealing between resonator end flanges and reservoir He tank. The outer liquid He tank surface is made of Ti, to better match the thermal conductivity of Nb and to reduce thermal stresses during cooling.

The Ti He tank is relatively large being adjusted to house not only SRFQ2, but SRFQ1 too, which is as large as SRFQ2 but twice longer. The tank weighs about 600 kg (resonator included) and contains about 600 l of liquid He, most of which fills the volume located under the resonator top.

A temperature floating, 1.6 mm thick, magnetic shield (CO-NETIC AA alloy Perfection) closes the He tank and the resonator ending plates reducing by a factor 10 the earth magnetic field inside the liquid He tank. A thin aluminized mylar sheet wraps the magnetic shield to reduce its emissivity. The cryostat thermal shield was originally designed to be cooled by He gas, but it was adapted to use liquid nitrogen, more easily available as a refrigerant. The cryostat vacuum tank is made of aluminum, but the large top flange, where all the feed-throughs are located, is made of stainless steel. A general view of the cryostat is presented in figure 2, its contents in figure 3.

As usual in heavy ion LINAC, there is no separation between the resonator and the cryostat vacuum, the only effective resonator outlet being the beam ports.

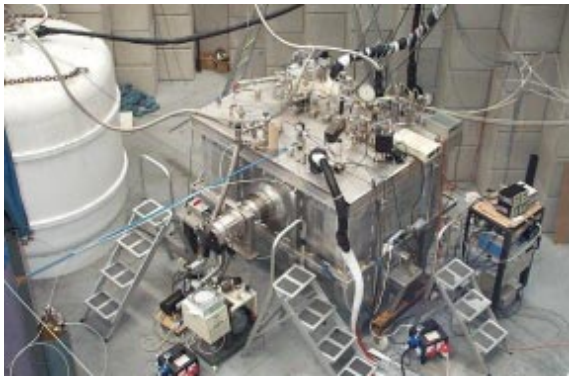

Figure 2. The test cryostat in the measurement hall.

Figure 3. SRFQ2 inside the test cryostat during transportation. An end plate of the nitrogen shield was removed for the He tank wrapped in a mylar sheet to be seen. At the center, where the magnetic shield is missing, a resonator end plate is visible.

3. SRFQ2 assembling

The SRFQ2 construction was completed in the beginning of 1999. After room temperature tests and a preliminary cooling at 77 K [14], the resonator was chemical treated at CERN where 60 μm from the inner surface were removed by a standard 1:1:2 bath (H_3PO_4, HF and HNO_3 respectively) [15]. Previously 60 μm had been removed from the stems before assembling the resonator.

At LNL there is no clean room to assemble the RFQ resonator in its test cryostat, so a protected space, slightly pressurized by filtered air, was prepared. A test cryostat was meantime adapted and assembled and the resonator ancillary equipment was designed and built [12].

After mounting the heaters and temperature sensors on the resonator, this is inserted in its LHe tank, closed by the magnetic shield and then wrapped in an aluminized mylar sheet. The He tank, which contains the resonator, is then pushed into the cryostat thermal shield and hung from the resonator top flange. Later the connections of the liquid He circuits are closed and vacuum tested.

The final resonator treatment is performed after having assembled the resonator on the cryostat; it foresees rinsing first with acetone and then with high-pressure water (HPWR). The resonator is then dried with ethanol and filtered air.

The antennas are then mounted and connected to their respective movement devices. The sputtered plates are mounted on the resonator ending flanges and the ports, for both antennas and the beam ports, closed to avoid contamination from dust. A few diodes, heaters and the tuners are mounted onto their respective resonator end plates. At this point the thermal shield has its lateral flanges closed, connected to the liquid nitrogen circuit and it is leak tested.

After moving the whole assembly onto the cryostat vacuum tank, the cryostat is evacuated very slowly in the initial stage to avoid movement of dust from the cryostat into the resonator inner surfaces.

As can be seen, the cryostat assembling is a complex procedure which takes weeks, but it is however possible, if necessary, to open and close the resonator end plates in few days (without disassembling the resonator from the He tank and from the cryostat top flange) for inspection or rinsing.

4. SRFQ2 cooling and conditioning procedure

A couple of days after closing the cryostat vacuum reaches to about 1×10^{-6} and the resonator baking begins. When, after about 24 h, the resonator temperature reaches 350 K, we start the thermal shield cooling. After about 36 more hours the heaters are turned off and the resonator temperature is left to drift. In a few days the temperature decreases to about 170 K.

In the mean time multipactoring conditioning is performed. It takes about 1 day to overcome all the levels which are reachable using the available 1 kW amplifier. Cooling to 4 K takes about 1 day and requires about 1500 l of LHe to fill the He reservoir.

The Q measurement at low field is performed measuring the stored energy decay time in critical coupling once the resonator temperature is stabilized and then the pick up antenna is calibrated. Multipactoring levels reachable only at 4 K have to be then conditioned. Under 20 kV inter-electrode voltages they form a continuous distribution, but at higher field the levels are of reactive type (typical tooth saw shape of the pick up signal) clearly well separated (at about 30, 45, 64, 90, 170 kV of inter-electrode voltage).

We start the multipactoring conditioning in CW, but, above 20–30 W forward power, it is necessary to operate in pulse mode in order not to cross the draining capability of the siphons. Too much gas, trapped inside the electrode, would lead to inefficient heat removal and would drive a normal conducting transition of the electrode.

The multipactoring conditioning time depends on resonator treatment; generally all levels are overcome in several hours.

At 90 kV we always start to see X-rays; initially they are very few, but they increase with the field level. Multipactoring and field emission processing have to go on in parallel and it is difficult to establish the contribution of each process to power dissipation.

The intensity of the radiation dose has been varied widely in the different measurement cycles. The maximum X-ray intensity was always localized just outside the cryostat in correspondence of resonator exit beam port. The maximum measured radiation level was 5 m SV/h, reached during high field conditioning (about 400 kV inter-electrode voltage reached feeding the cavity in pulsed way by 1 kW pulsed power with a duty factor of about 5%). Both rf and He process conditioning are useful to increase the resonator performance, the second proving to be more effective, but potentially more dangerous. Usually we begin with rf conditioning and, only after having measured the first Q curve, we start some hours He conditioning. We inlet pure He gas in the cryostat vacuum until the pressure, measured by an ionization gauge located on the cryostat top flange, increases to no more than about 1×10^{-6}. It is difficult to determine what is the vacuum inside the resonator in such a condition and so we pay attention to avoid rf discharge (very fast vanishing of the pick up signal) in the resonator.

Figure 4. The mechanical tuner mounted on its end plate. The pushers, which allow a good electric contact between cavity body and plate without any gasket, are visible on the plate border.

At the end, after restoring good vacuum in the cryostat (we arrive in 10^{-8} mbar scale), we check again the resonator performance. Usually both the flat part of the Q curve and the radiation intensity onset, shift to higher voltage, as the X-ray production is reduced.

5. Evolution of SFQ2 performance

SRFQ2 was subjected to a few measurement cycles in 2000–2001. We wish to recapitulate them historically hereafter.

At the end of 1999 the stuck of the power coupler antenna, in a strongly over-coupled position, prevented the possibility of determining the resonator Q. We then decided to make the coupler movement more reliable, redesigning the line completely. We removed the gasket, which was meant to act as a thermal joint between the end plates and the cavity body on February 2000. As a matter of fact the associate rf losses had previously limited the resonator Q to 5.7×10^6. The suspicion of too high gasket power dissipation was confirmed lowering the cavity temperature to 2.6 K, by pumping on the He bath: in that condition there was an increase of the cavity low field Q to 6×10^7.

In the new design the sputtered plates are forced to touch directly the resonator body by pushers (76 each) equally spaced all around the plate circumference (figure 4). We think that the Nb sputtered copper plates help in realizing good contacts, especially because the nitride of the Nb film creates a column structured film surface, which makes it easier to brake the surface oxide on the cavity side. The importance of producing good and uniform contacts was confirmed in February 2001 when the removal of only 8 pushers in each plate lowered the resonator Q_0 from 8×10^8 to 5×10^7.

In May 2000 the cavity reached a Q_0 of 8×10^8. The Q switched then to a value of 6×10^8 remaining constant up to about 90 kV. During conditioning, a failure in the input rf line stopped the measurement. The cause was a discharge started by a small wire of the outer conductor protruding towards the inner conductor in a cable connector.

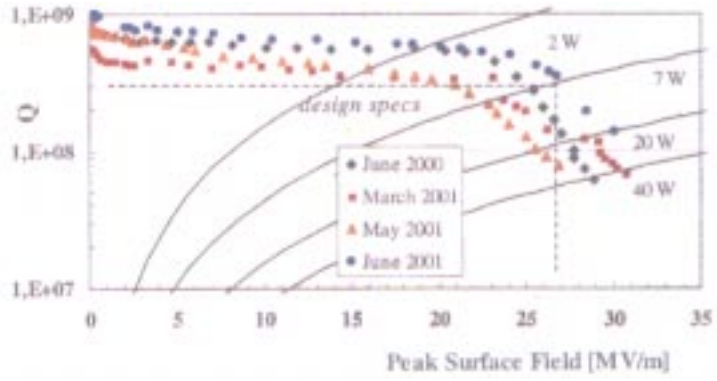

Figure 5. The best Q measurement obtained between 2000 and 2001 in SRFQ2 resonator.

The cavity reached for the first time the design performance (280 kV inter-electrode voltage at 7 W dissipated power that means 25.5 MV/m peak surface electrical field) in May 2000. In this test the Q curve remained flat at a Q value of about 6×10^8 up to 250 kV, where it bent because of field emission process associated to X-ray production. The best Q curves obtained in the first half of 2001 test are shown in figure 5 with the final June 2000 curve.

A cold leak, which ended up to be located in the copper gasket of a titanium resonator flange, delayed further rf tests till the beginning of 2001. Once the cause of the leak was found, all the copper gaskets on the titanium flange were substituted by indium joint to avoid problems in the future.

The lower Q value in March 2001 with respect to June 2000 is probably due to the repeated opening of the cryostat, while looking for the cold leak, without a final HPWR. The inter-electrode voltage reached anyway a maximum CW value of 300 kV. Further conditioning leaded however to discharges that limited the maximum inter-electrode voltage to 250 kV. A decrease of Q_0 to 3.5×10^8 was also registered.

Later, on opening the cryostat, we found dust around, in particular on the electrode located under the antennas: their outer conductor sliding contacts lead to scratching of the outer connection and created the dust which fell down onto the electrodes. This was probably the reason of the strong field emission, noticed during March 2001 test, which long rf and He conditioning could shift to high fields but never eliminate completely.

To avoid dust collecting on the electrodes, the antennae will be mounted from the resonator bottom in the line cryostat. Meantime a change in the antenna design, implemented before the fall test, helped in preventing further dust falling in the test cryostat.

The SRFQ2 Q_0 value improved again in May 2001, after HPWR. Conditioning helped to straighten the curve up to 200 kV, where it bent, limited by field emission associated to X-ray production. Lack of LHe did not allow further conditioning. In the following cooling cycle in June 2001, performed without breaking the cryostat vacuum, four hours He conditioning helped to improve Q_0 to 7×10^8, to flaten the curve and to shift the field emission onset to 240 kV inter-electrode voltage.

However, after setting the power coupler for amplitude and locking test, there was an anomalous power consumption, which was not correlated to any temperature increase of

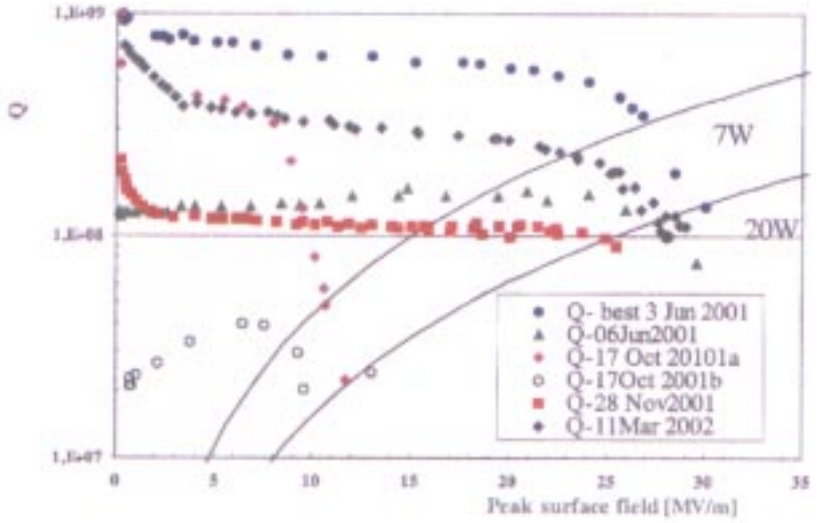

Figure 6. Evolution of the SRFQ2 performance. The best results were obtained in June 2001 (full circle), but sputtering of Cu and SS from the coupler antenna during high power test leaded to the June 6th curve (triangles). The *Q* performance at low field recovered in October 17th (diamonds), but it was soon spoiled during He conditioning (empty circle). In the last measurement of November 2001 (squares), after an initial decay at low field, the *Q* curve remained constant up to design voltage, but at an increased power consumption.

the cavity sensors. The *Q* curve that resulted showed a lower Q_0 value of about 2×10^8, straight up to 250 kV, but with a puzzling positive drop, as can be seen in figure 6. The inter-electrode value of 280 kV required 15 W dissipated power. After removing the resonator end plates at the end of the measurement, the reason for the bad performance was found to be due to copper and stainless steel contamination of the cavity surface around the power antenna. A loose contact in its outer conductor cable produced the conditions for a sputtering process, when the antenna was fed in the presence of He during conditioning. The contamination was removed by 3M scotch brite lapping, followed by standard HPWR.

In spite of scratches present on the treated area, in the following October 2001 test, Q_0 reached a value of 1×10^9; a few hours rf conditioning led to the curve 'October 2001a' in figure 6, where strong field emission is present at highest reached inter-electrode voltage (about 100 kV). It was not possible to overcome this value without having discharges associated to an increase of the temperature of the horizontal electrode, which was never present earlier. He conditioning did not help, but instead spoiled further the *Q*, as evident in figure 6 (curve 'October 2001b'). Opening the resonator we found spots on the electrode tips, especially in one of the output electrode ends. The images of the two electrode ends were evident on the related end plate (figure 7).

Brownish shadows had been increasing on the plates with each test, but for the first time there was a shining border, shaped as the end of electrodes, where the shadow was completely removed and the Nb seems to have a different structure. The plates, which were in use since the first test, were changed with new units.

Figure 7. High voltage electrode end images on the output plate.

Lapping by 3M Imperial aluminum oxide film eliminated the spots from outer electrodes end surface. This process left aluminum oxide on the treated surface, but it allowed to continue the resonator characterization without waiting a long time, which would have been required by a chemical treatment.

In the following November 2001 test the Q curve recovered with respect the October ones, but the Q_o was limited to 1×10^8. A fast conditioning helped to flatten the Q curve up to 300 kV practically without having field emission. The X-ray dose rate remained below the 10 m Sv/h up to the highest reached fields. The design voltage could be obtained at the price of higher power consumptions (20 W instead of 7 W), but there was finally a possibility of the cavity characterization described in the following paragraph.

6. Resonator behavior, stability and locking test at 4 K

The determination of SRFQ2 resonant drifts as a function of change in He bath pressure, mechanical noise and radiation pressure is very important because the resonator has to operate locked in phase and amplitude [16,17].

A systematic analysis of the influence of all these parameters was performed in November 2001, after obtaining a flat Q curve.

The variation in frequency as function of He bath pressure level is presented in figure 8.

A pressure increase over the He bath produces a reduction of resonance frequency of about 40 Hz/mbar, which is quite high in comparison to Legnaro full Nb QWR resonators, which have a sensitivity of 1 Hz/mbar. The cryogenic system feeding the RFQ cryostat works at a pressure of 1.2 bar $\pm$50 mbar, but guarantees changes lower than 2 mbar/min, which are small enough to be easily adjusted by slow tuner devices.

The SRFQ2 has a mechanical tuner, connected to a stepping motor, in each of the two end plates.

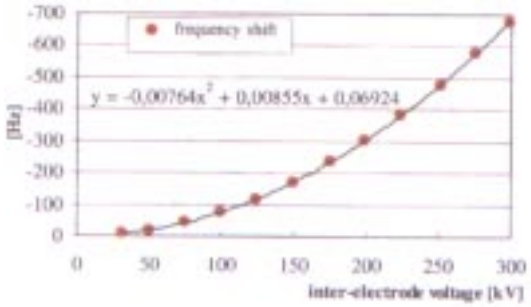

Figure 8. Frequency shift induced by He bath pressurization.

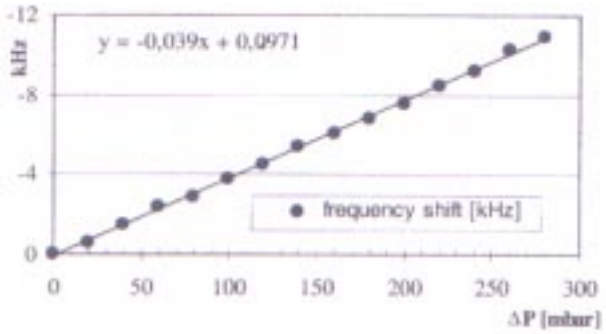

Figure 9. SRFQ2 resonance frequency shift as a function of the inter electrode.

The total tuning range is 300 kHz and the sensitivity is about 0.5 Hz/step. The backlash is very reproducible (about 500 step, depending on the plate position) and it is possible using only one of them, as in the full Nb Legnaro QWRs.

Probably it is more reliable to push one of them to increase the frequency and pull the other to decrease it, thus avoiding having to recover the backlash in case of change of direction.

The resonator frequency decreases quadratically as a function of the inter-electrode voltage (figure 9) being due to Lorentz detuning. The frequency change is strong in this structure where, due to the positioning of the stems, the current travels in the four electrodes in the same direction leading to a magnetic attractive force, which squeezes the electrodes producing a capacity increase and, consequently, a decrease in resonant frequency.

This effect causes a steering of the resonance curve, as it is possible to see in figure 10. It has been obtained by measuring the resonator frequency and field amplitude, when the phase in the phase shifter present in the close loop feeding the cavity [17] was changed. The SRFQ2 inter-electrode voltage was set at 198 kV at resonance and with a resonator loaded Q of 4.6×10^6.

It is possible to notice that, applying the correction for Lorentz detuning, as computed by the data presented in figure 9, the curve approaches the theoretical one. It is interesting to notice that the best fit is obtained when a simple quadratic correction of $\delta f = -0.0085$ Hz/(kV)^2 is applied.

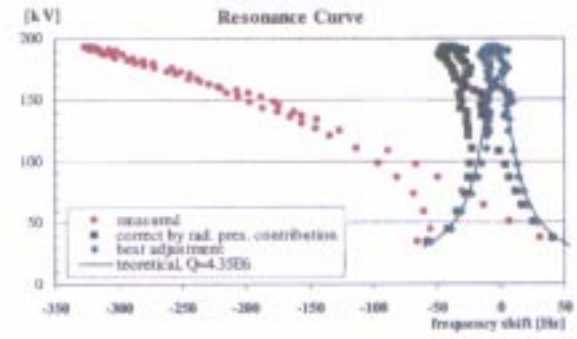

Figure 10. Steering of the resonance (circles). The curve assumes its theoretical shape (black line) if the measured frequency shifts are corrected by the Lorentz detuning contribution.

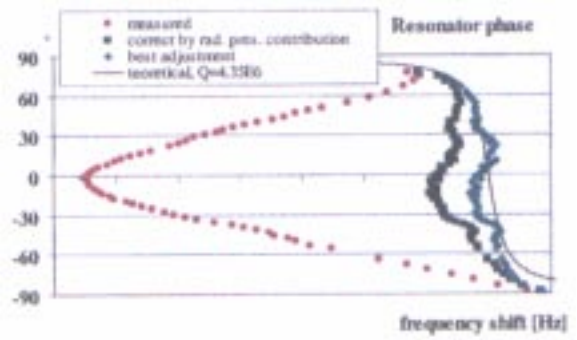

Figure 11. Steering of the resonator phase (circles). The curve assumes its theoretical shape (black line) if the measured frequency shifts are corrected by the Lorentz detuning contribution.

Plotting the opposite of the set loop phase as a function of the measured shifts in frequency leads to the phase plot presented in figure 11.

Applying the correction due to Lorentz detuning to the measured frequency shifts, the experimental curve approaches the theoretical one.

Again the best fit is obtained by a simple quadratic correction ($\delta f = -0.008\,5\text{Hz}/(\text{kV})^2$).

In figure 12, the drift in frequency, while operating the resonator at 220 kV for about 6 h, is presented. In the plot very fast spike of about 20 Hz at every $7'30''$ are present. They did not appear in a similar test in July 2001 [16] and they are clearly connected to a periodic noise present in the test room to which our measurement system is sensitive. We hope to eliminate it next time or at least to reduce the sensitivity of our measurement system to it.

Excluding these spikes the shifts in frequency are very limited: a few Hz on 20 to 30 s period, superimposed on a slower drift leading to a total of 100 Hz in 2 h. Similar plots were registered in other conditions.

In spite of the frequency spikes, the resonator phase and amplitude locking was possible a few times for tens of minutes each at an inter-electrode voltage up to 200 kV, working practically on resonance (at the phase which produces the maximum voltage which is an

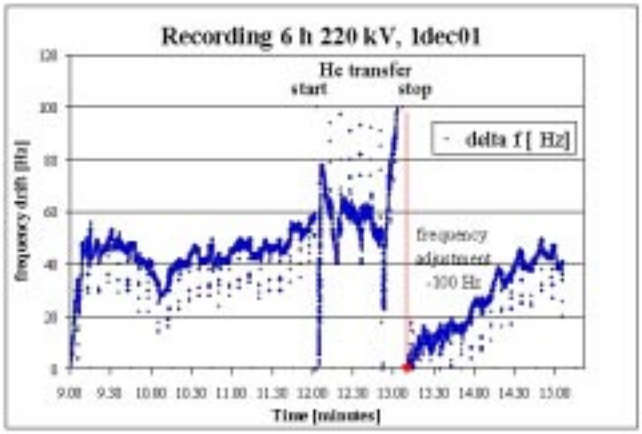

Figure 12. Recording of the resonator frequency drifts. At every $7'30''$ spikes are present.

unstable point because of radiation pressure) and with a loaded Q of 4.3×10^6. The attention devoted in pushing to high frequency the lowest mechanical resonance in the resonator design seems to work properly.

We are confident that it will be possible to operate SRFQ2 at the design field, when working out of resonance (on the right side of the resonance curve) and when setting the soft tuners parameters properly.

7. Conclusion

A final test on SRFQ2 is planned in the test cryostat at the end of January 2002 to set the slow tuner parameters and to complete the locking procedure. Further tests of SRFQ2 after the assembling of the fast tuner device, built in collaboration with Argonne will be possible only after the arrival of the operation cryostat in the spring of 2002.

In this period we will start tests on SRFQ1, now completed, and by the end of the year both resonators should be mounted on their common final cryostat and put on PIAVE line for beam test.

References

[1] A Pisent *et al*, *Proc. EPAC98*, Stockholm, 22–26 June 1998 (Institute of Physics Publishing, Bristol and Philadelphia) pp. 1840–1842
[2] A Lombardi *et al*, *Proc. LINAC 2000*, pp. 356–360
[3] A Dainelli *et al*, *Nucl. Instrum. Methods* **A382**, 100 (1996)
[4] M Cavenago, T Kulevoy and S Petrenko, *Proc. EPAC 2000*, Vienna, Austria, June 2000, p. 2417
[5] A Facco and V Zviagintsev, *Proc. 9th RF Superconductivity Workshop*, Santa Fe, New Mexico, LA-13782-C, 1999, pp. 203–206
[6] V Andreev, G Bisoffi, M Comunian, A Lombardi, A Pisent, A M Porcellato and T Shirai, *Proc. XIX International Linear Accelerator Conference*, Chicago, Il, USA, 23–28 August, pp. 965–967

[7] A Pisent, M Cavenago, P Bezzon, S Canella, F Cervellera, M Comunian, A Facco and A Lombardi, *Proc. EPAC 2000*, Vienna, Austria, June 2000, p. 1702
[8] G Bisoffi *et al*, *Proc. 8th International Conference on Heavy Ion Accelerator Technology*, Argonne, 4–11 October 1998, *AIP Conference Proceedings 473*, 1999, p. 173
[9] G Bisoffi, *Design of a superconducting RFQ*, LNL-INFN (REP) 154/2000
[10] A Pisent, *Proc. 8th International Conference on Heavy Ion Accelerator Technology*, Argonne, October 1998, p. 214
[11] S Stark, V Palmieri, L Badan, V Durand, I I Kulik and R Preciso, *Proc. 8th Workshop on RF Superconductivity,* Abano (Pd) Italy, October 1997, p. 1156
[12] F Chiurlotto, L Bertazzo, G Bisoffi and A M Porcellato, *Proc. 8th Workshop on RF Superconductivity*, Abano (Pd), Italy, October 1997, p. 615
[13] A Lombardi *et al*, *Proc. 1999 Particle Accelerator Conference*, New York, 1999, p. 1324
[14] G Bisoffi, V Andreev, G P Bezzon, F Chiurlotto, A Lombardi, V Palmieri, A M Porcellato, S Stark and E Chiaveri, *Proc. 9th Workshop on RF Superconductivity*, Santa Fe, New Mexico USA, 1–5 November 1999, p. 367
[15] G Bisoffi *et al*, *Proc. EPAC2000*, Vienna, Austria, June 2000, p. 324
[16] G Bisoffi *et al*, *Proc. 10th Workshop on RF Superconductivity*, Tsukuba City, Japan (in press); on web @http://conference.kek.jp/SRF2001/index.htlm
[17] G Bassato, A Battistella, M Bellato and S Canella, *Nucl. Instrum. Methods* **A328**, 195 (1993)